Atmos. Chem. Phys., 10, 11305–11322, 2010
www.atmos-chem-phys.net/10/11305/2010/
doi:10.5194/acp-10-11305-2010
© Author(s) 2010. CC Attribution 3.0 License.

Atmospheric Chemistry and Physics

The relative importance of various source regions on East Asian surface ozone

T. Nagashima[1], **T. Ohara**[1], **K. Sudo**[2,3], **and H. Akimoto**[4]

[1]Asian Environment Research Group, National Institute for Environmental Studies, Tsukuba, Japan
[2]Graduate School of Environmental Studies, Nagoya University, Nagoya, Japan
[3]Research Institute for Global Change, Japan Agency for Marine-Earth Science and Technology, Yokohama, Japan
[4]Asia Center for Air Pollution Research, Niigata, Japan

Received: 4 March 2010 – Published in Atmos. Chem. Phys. Discuss.: 9 April 2010
Revised: 10 October 2010 – Accepted: 8 November 2010 – Published: 30 November 2010

Abstract. We estimated the source-receptor relationship for surface O_3 in East Asia during the early 2000s using a method that tags O_3 tracers according to their region of chemical production (tagged tracer method) with a global chemical transport model. The estimation demonstrated the importance of intracontinental transport of O_3 inside East Asia as well as of the transport of O_3 from distant source regions. The model well simulated the absolute concentration and seasonal variation of surface O_3 in East Asia and demonstrated significant seasonal differences in the origin of surface O_3. In the cold season (October to March), more than half of surface O_3 in East Asia is attributable to the O_3 transported from distant sources outside of East Asia. In the warm season (April to September), most of the surface O_3 is attributable to O_3 created within East Asia in most areas of East Asia. In spring the contribution of domestically created O_3 accounted for 20% of the surface O_3 in Japan and the Korean Peninsula, 40% in the North China Plain, and around 50% in the southern part of China, and the domestic contribution increased greatly in summer. The contributions of O_3 created in China and the Korean Peninsula to O_3 in Japan were estimated at about 10% and 5%, respectively. We also demonstrated a large contribution (20%) from China to the Korean Peninsula. In the northern and southern parts of China, large contributions of over 10% from East Siberia and the Indochina Peninsula, respectively, were identified. The contribution from intercontinental transport increased with latitude; it was 21% in Northeast China and 13% in Japan and the Korean Peninsula in spring. As for the hourly mean of surface O_3, domestically created O_3 was the main contributor in most areas of East Asia, except for the low O_3 class (<30 ppbv), and accounted for more than 50% in the very high O_3 class (>90 ppbv). The mean relative contribution of O_3 created in China to O_3 in central Japan was about 10% in every class, but that created in the Korean Peninsula was significant in all except the low O_3 class. We identified the substantial impact of foreign sources on Japan's ambient air quality standard in the high O_3 class (60–90 ppbv) in spring.

Correspondence to: T. Nagashima
(nagashima.tatsuya@nies.go.jp)

1 Introduction

Tropospheric ozone (O_3) near the Earth's surface can be a harmful atmospheric pollutant since high levels of O_3 can have detrimental effects on human health (US Environmental Protection Agency (US EPA), 2006) and cause biochemical damage to plants, reducing the primary productivity of plants and crop yields (Kobayashi, 1999; Wang et al., 2005; US EPA, 2006). It is now well established that the concentration of surface O_3 in a given region is controlled through a balance between transport from outside of the region, including other continents and the stratosphere, dry deposition onto the surface, and photochemical reactions, involving nitrogen oxides (NO_x = NO+NO_2), carbon monoxide (CO), and volatile organic carbons (VOC) on a local and regional scale (Brasseur et al., 1999; Stevenson et al., 2006; Wild, 2007). Intense emissions of these precursors of O_3 (NO_x, CO, and VOCs) from industrial activities, electrical power generation, and road transportation cause photochemical smog around big cities and industrial regions. Japan experienced severe photochemical smog associated with economic growth and motorization in the early 1970s, followed by a remarkable

Published by Copernicus Publications on behalf of the European Geosciences Union.

improvement of the air quality in the subsequent decade due to the enactment and gradual reinforcement of regulations against emissions of O_3 precursors. Since then, concentrations of non-methane hydrocarbons (NMHCs) over Japan have been continuously decreasing, and NO_x concentrations remained almost constant during the 1980s and 1990s, followed by a decrease after 2000 (MOE Japan, 2008). In spite of these facts, long-term monitoring data shows that the surface concentration of O_3 in Japan resumed its increase in the mid-1980s and has continuously increased until the present time (Ohara and Sakata, 2003). This increase in surface O_3 has been observed over almost the entirety of Japan, including remote monitoring sites located on mountains or islands where no major sources of O_3 precursors exist (Ohara and Sakata, 2003; Tanimoto, 2009). These observed features of air quality in Japan strongly suggest that the recent increase in O_3 cannot be solely attributed to local pollution as in the early 1970s but is influenced by the transport of O_3 from outside of Japan.

Regarding other East Asian countries, researchers have observed an increasing trend in O_3 concentration in mainland China, Hong Kong, and Taiwan (Chou et al., 2006; Lu and Wang, 2006; Chang and Lee; 2007, Xu et al., 2008; Wang et al., 2009), implying that the increase in O_3 is an issue for the entire East Asian region. The estimated increase in anthropogenic emissions of O_3 precursors in East Asian countries during the last two decades (Ohara et al., 2007), which was also inferred from the space-based measurement of an increase in tropospheric column NO_2 (Richter et al., 2005; Irie et al., 2005), is likely a major cause of the observed increase in East Asian O_3. However, the influence of O_3 precursors emitted in regions outside of East Asia and of stratospheric O_3 on the observed increase in East Asian O_3 should not be ruled out because sufficient knowledge of the relative importance of each source region of O_3 on the amount of O_3 over the East Asian region is unavailable. Therefore, before discussing the causes of the recent increase in East Asian O_3, quantitative estimation of the amount of O_3 that is transported into East Asia from outside sources as well as the amount of O_3 transported intracontinentally among the East Asian countries is required.

Such quantitative estimations of the proportion of O_3 over a receptor area that can be attributed to a source region, the so-called source-receptor (S-R) relationship for O_3, have been widely studied (Wang et al., 1998; Jacob et al., 1999; Wild and Akimoto, 2001; Fiore et al., 2002; Li et al., 2002; Derwent et al., 2004; Wild et al., 2004; Auvray and Bey, 2005; Sudo and Akimoto, 2007). Moreover, the United Nations Economic Commission for Europe (UNECE) Convention in Long Range Transboundary Air Pollution (CLRTAP), the Task Force on Hemispheric Transport of Air Pollution (TF HTAP) (Keating and Zuber, 2007; Fiore et al., 2009) has been conducting an internationally coordinated effort to quantify and estimate uncertainties in the S-R relationship for O_3 and other air pollutants. However, many of these studies focus on the intercontinental transport of O_3 between the highly populated and industrialized regions in the mid-latitudes of the Northern Hemisphere, i.e., North America, Europe, and Asia, and pay little attention to the intracontinental transport of O_3.

There are a few studies addressing the S-R relationship for O_3 in Asia. For instance, Li et al. (2008) studied source apportionment of O_3 observed at Mt. Tai in central eastern China during a field campaign carried out in June 2006 (Kanaya et al., 2009) using a regional chemical transport model. They estimated contributions from defined source regions, which are closely partitioned within China, to the O_3 amount at Mt. Tai. However, a one-month estimation at only one particular receptor point cannot provide the whole picture of the S-R relationship for O_3 in the East Asian region. The S-R relationship for acidifying species over a longer timeframe has already been estimated for sulfur deposition (Carmichael et al., 2002; Lin et al., 2008), but for O_3, such estimations of the S-R relationship have yet to be reported.

In this study, we estimated the S-R relationship for O_3, in particular for surface O_3, in East Asia based on a previous study by Sudo and Akimoto (2007), which demonstrated the significant role of intercontinental transport of O_3 on the global distributions and budgets of tropospheric O_3, using the tagged tracer method with a global chemical transport model. Our current study further investigated contributions from various source regions to the East Asian O_3 concentrations, taking into account both the intracontinental and the intercontinental transport of O_3. We performed the estimation based on a multiyear simulation over the early 2000s, using a global-scale chemical transport model with the tagged tracer method, to obtain an averaged picture of the S-R relationship for O_3 in recent years. In the next section, a brief description of the model and experimental method are presented. The model simulation is evaluated against observations at surface monitoring sites, and the simulated contributions from various source regions are then discussed in the Results section. The difference in estimated contributions, depending on the class of hourly surface O_3 concentrations, is also discussed in the Results section.

2 Methods

There are two major approaches used to quantify the contributions of the source regions of O_3 to the amount of O_3 in a receptor area. One is the emission sensitivity approach, which performs two simulations: a perturbed run with and a standard run without a perturbation in the O_3 precursor emission, respectively, of the designated source region or source sector, to obtain the contribution of that source to O_3 in a receptor region by taking the difference of calculated O_3 between the two runs (Jacob et al., 1999; Wild and Akimoto, 2001; Wild et al., 2004; Fiore et al., 2009). The second approach is the tagged tracer method, which calculates the

distribution of hypothetical O_3 tracers, each of which is allowed to be chemically produced only inside its designated source region. Then, the concentration of each O_3 tracer tagged by its source region represents the contribution of that source region. This method has been used in many studies addressing a wide variety of issues using both global and regional chemistry transport models (Wang et al., 1998; Fiore et al., 2002; Auvray and Bey, 2005; Sudo and Akimoto, 2007; Li et al., 2002, 2008).

The emission sensitivity approach estimates the amount of O_3 in a receptor region that is produced by, and is thus attributable to, the precursors of O_3 emitted inside each source region irrespective of the location they were chemically converted to O_3. In contrast, the tagged tracer method calculates the amounts of O_3 in a receptor area that was chemically produced inside each source region and then transported to that receptor area, inevitably including quantities of O_3 created inside a source region from precursors emitted in adjacent source regions and transported to that source region. Therefore, the S-R relationships for O_3 estimated by these two approaches can differ. Li et al. (2008) compared the two methods for the contribution of high O_3 production regions in China to the O_3 concentration at Mt. Tai in June 2006 and found that the difference could be as much as 30%. They concluded that both approaches agreed reasonably well with each other. Although this example does not guarantee consistency between the approaches, we decided to employ the tagged tracer method in this study mainly because of its computational efficiency. This study aimed to estimate the mean contributions from many source regions (number of regions $N > 20$) separately with multiyear model simulations. To achieve this, the emission sensitivity approach requires $N+1$ runs to deduce the contribution of each source region for a single year, whereas the tagged tracer method requires only two runs for a single year using the framework described in the following section.

2.1 Model description

We used a chemistry climate model for the troposphere, CHASER (Sudo et al., 2002a). CHASER was developed based on the atmospheric component of a coupled general circulation model, MIROC, developed by the Center for Climate System Research (CCSR), the National Institute for Environmental Studies (NIES), and the Frontier Research Center for Global Change (FRCGC) (Numaguti et al., 1995; K-1 Model Developers, 2004). The framework of the model is almost identical to that used in a previous study by Sudo and Akimoto (2007), hereafter referred to as SA07. However, to better resolve individual Asian countries, this study uses a finer horizontal grid spacing (T63: approximately 1.9° by 1.9° in longitude and latitude) than previously used (T42: approximately 2.8° by 2.8°), since the aim was to investigate the intracontinental as well as the intercontinental transport of O_3. The top layer of the model was set at an altitude of about 40 km with 32 vertical layers. The model calculated the concentrations of 53 chemical species through 27 photolysis and 113 chemical reactions, representing a detailed tropospheric chemistry involving the O_3-HO_x-NO_x-CH_4-CO system and oxidation of NMHCs. The model also included the sulfate formation process with gas and liquid phase oxidation of SO_2 and dimethyl sulfide (DMS). A dry deposition scheme based on the resistance series parameterization of Wesely (1989) and two different processes of wet deposition (in-cloud and below-cloud scavenging) were also included. For dry deposition, we introduced the reduction of deposition at a lower temperature that is described in the original literature of the parameterization by Wesely (1989) in order to reduce the underestimation of surface O_3 in the northern part of Japan. The advective transport of chemical species was calculated with a fourth-order flux-form advection scheme of the monotonic van Leer (van Leer, 1997) and the flux-form semi-Lagrangian advection scheme of Lin and Rood (1996). Vertical transport by moist convection was also considered in the cumulus convection process, which is based on the Arakawa-Schubert scheme (Emori et al., 2001). The concentrations of O_3 and some nitrogen compounds (NO_x, HNO_3, N_2O_5) above the tropopause were assimilated into the monthly mean output data of the stratospheric chemistry climate model. The data for the assimilation was taken from Akiyoshi et al. (2009) for O_3 as it represented the interannual variation of stratospheric O_3 in the last couple of decades and from Takigawa et al. (1999) for the nitrogen compounds (climatological data).

In this study, we used two different setups of CHASER: a full-chemistry setup and a tracer-transport setup. The full-chemistry setup calculated the temporal evolution of the chemical species through the actual chemical-physical procedure as mentioned above whereas the tracer-transport setup calculated the temporal evolution of hypothetical O_3 tracers with archived chemical tendencies. The detailed calculation procedure is described in the next subsection.

2.2 Tracer tagging

The tracer tagging method used in this study consisted of two steps (Sudo and Akimoto, 2007). First, we performed a standard simulation with the full-chemistry setup of CHASER to archive 3-hourly mean 3D fields of chemical production (P) and loss frequencies (L) of the extended odd oxygen family (O_x = O_3+O+O(^{1}D)+NO_2+2NO_3+3N_2O_5+PANs+HNO_3+other nitrates). We used P and L of the O_x family instead of those of O_3 to eliminate the rapid null cycles within the O_x family, as in previous studies (Wang et al., 1998; Li et al., 2002; Fiore et al., 2002). The standard simulation also output the daily 3D distribution and hourly surface concentration of O_3, which are hereafter referred to as the "total" O_3. Note that this O_3 data is a sum of O_3, O, and O(^{1}D). Since the concentrations of O and O(^{1}D) are both negligible in the

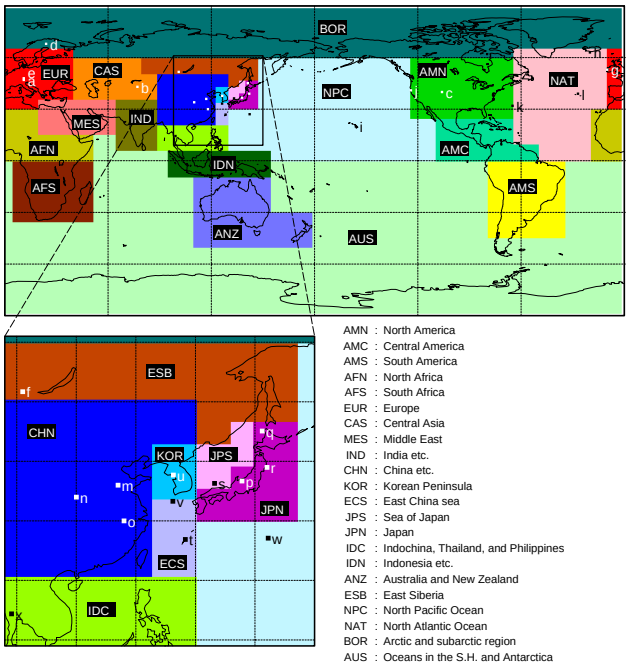

Fig. 1. Horizontal definition of source regions used to tag O_3 tracers. This horizontal separation is applied for both the PBL and the FT. The East Asian region is expanded for clarity. Marked solid squares and letters next to them indicate the locations for which the comparisons between observations and model calculations are shown in Fig. 2.

troposphere compared to that of O_3, we refer to the output data as O_3 for the sake of brevity. The standard simulation was then followed by a second simulation, which used the tracer-transport setup of CHASER. In the second simulation, we calculated the temporal evolution of the hypothetical O_3 tracers, each of which was assigned to a particular region in the model domain (Fig. 1). The assignment of a tracer to each region was done in the following manner. The transport and dry deposition of each tracer were calculated in the same way as in the standard simulation, but the chemical evolution of tracers was calculated using the archived P and L of O_x. Each O_3 tracer could be lost chemically at the frequency of L everywhere in the model domain, but it could be produced chemically only inside its assigned source region. In the stratosphere, the concentration of O_3 tracer assigned to the stratosphere was assimilated into the same stratospheric O_3 data as used in the standard simulation, but those of the tracers assigned to the region in the troposphere were all set to zero. In SA07, the O_3 tracer assigned to the stratosphere was assimilated only above 55 hPa altitude to avoid the non-negligible contribution of O_3 and the precursors transported from the troposphere to the lower stratosphere. However, we did not employ that procedure in the present study. Instead, we assimilated the O_3 tracer assigned to the stratosphere over the tropopause defined by the lapse rate; otherwise, the concentrations of total O_3 in the upper troposphere would be overestimated. Hess and Lamarque (2007) introduced a different procedure to deduce the stratospheric contribution, which was based on tagging the tropospheric emission of NO_x, giving qualitatively different results from that given by the method employed in this study. In the Northern Hemisphere, the stratospheric portion of surface O_3 obtained using the method of Hess and Lamarque (2007) is generally smaller than that using the current method. They argued that their method had some conceptual advantages over the current method, but there has not been a consensus on which method is better for estimating the stratospheric contribution. The concentration of each O_3 tracer tagged via its assigned source region was then scaled so that the sum of all tagged O_3 tracers equaled the total O_3 output by the standard simulation. The resultant concentration of each tagged O_3 tracer at a given location represents the contribution of O_3 that was created in each source region and transported to that location.

For the tracer tagging, we separated the model domain into 45 regions, which included 22 regions both in the planetary boundary layer (PBL) and in the free troposphere (FT), as shown in Fig. 1, as well as one whole stratosphere. As to the vertical classification between the PBL and the FT, SA07 defined the PBL as the six lowermost layers in the model (surface to about 750 hPa), based on the observed and modeled vertical profiles of O_3 production. We adopted the same procedure to separate the PBL from the FT. We applied the same horizontal separation of source regions depicted in Fig. 1 in the PBL and the FT. This horizontal separation was different from that applied in SA07, in which different horizontal separations for the PBL and the FT were employed and most of the oceans and East Siberia were assigned to one source region. In this study, since special focus was placed on the intracontinental transport of O_3 inside East Asia, we further separated the source regions in East Asia; the Korean Peninsula, the Sea of Japan, and the East China Sea were separately defined. We also set source regions for the North Pacific Ocean and the North Atlantic Ocean separately because our pilot simulation showed that both regions had non-negligible contributions to the East Asian surface O_3 and should be considered independently of each other.

2.3 Experimental design

We modeled simulations for six years from 2000 to 2005. The model meteorology (horizontal wind velocities and temperature) was assimilated into the National Center for Environmental Prediction/National Center of Atmospheric Research (NCEP/NCAR) 6-hour reanalysis data (Kalnay et al., 1996) of the corresponding year. Sea surface temperature and sea ice data used in the model were taken from the Hadley Centre's Sea Ice and Sea Surface Temperature data set (HadISST) (Rayner et al., 2003). For the first step of the full-chemistry calculation, we used the following

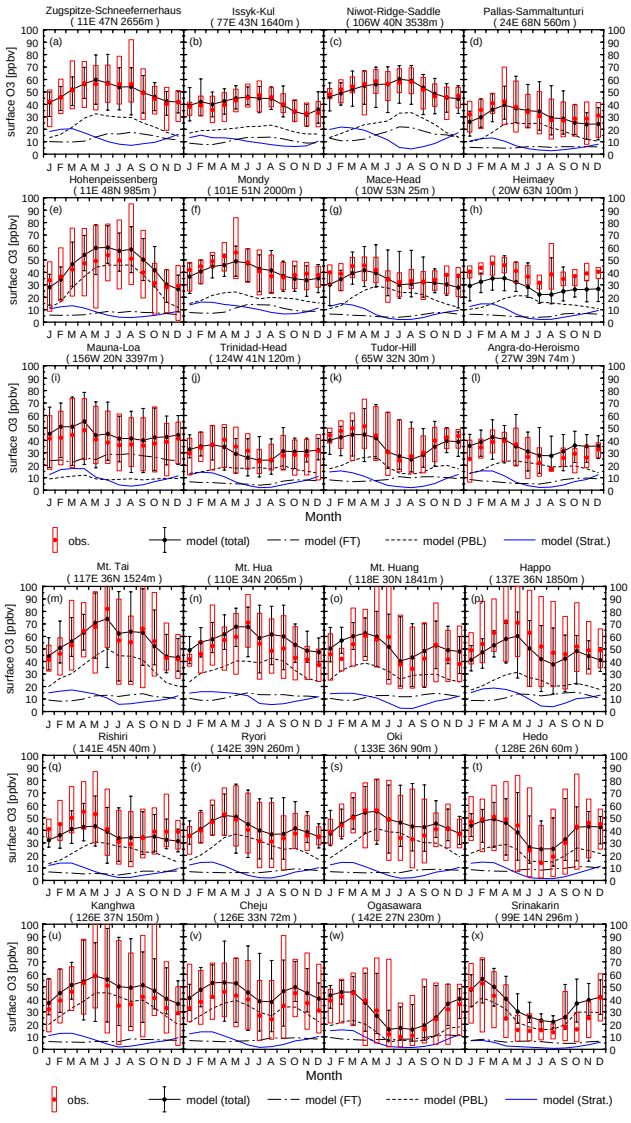

Fig. 2. Seasonal variations of the monthly mean surface O_3 observations (red filled circles) and model calculations (black circles and thick black solid lines), with contributions from the stratosphere (blue solid lines), PBL (black dashed lines), and FT (black dash-dotted lines), calculated by the model. Monthly means and each contribution are multiyear (6 years for the model and available years for the observations) averaged values. Vertical bars and boxes denote the multiyear range of the daily mean surface O_3 for each month for the model and the observations, respectively. Model calculations are interpolated to the longitude, latitude, and altitude of the location of each site.

emission data sets of O_3 precursors (NO_x, CO, NMHCs) from various origins. Anthropogenic emission data were from the latest version of the Regional Emission inventory in Asia (REAS ver.1.2) (Ohara et al., 2007) for the Asian region and the Emission Database for Global Atmospheric Research Version 3.2 (EDGAR3.2) Fast Track 2000 (FT2000) data (Olivier and Berdowski, 2001) for the rest of the world. For O_3 precursor emissions from biomass burning, we adopted vegetation fire emission data compiled for the REanalysis of the TROpospheric chemical composition over the past 40 years project (RETRO) (Schultz et al., 2008) for the whole land area. Note that REAS emission data for each year from 2000 to 2005 was available but EDGAR3.2 FT2000 and RETRO data for the year 2000 was used for every year. We also considered natural sources of NO_x from soil (5.5 TgN/yr) and lightning (3.3 TgN/yr). Large biogenic emissions of isoprene (400 TgC/yr) and terpenes (100 TgC/yr) were used following SA07. We took the initial condition of the simulation from a 5-year integration using CHASER with constant boundary conditions for the year 2000, which was long enough to obtain the equilibrium state.

3 Results

3.1 Model evaluation with surface O_3 observations

The ability of CHASER to represent the observed concentrations of O_3 and the related chemical species has been validated in previous studies (Sudo et al., 2002b; Sudo and Akimoto, 2007). However, we employed a finer horizontal resolution than used in previous studies and the emission data of the O_3 precursors and the driving meteorological field were updated for the current study. Thus, the current model setup of CHASER should be re-validated, particularly against the new observations coincident with the period of model simulation (2000 to 2005).

Figure 2 shows the comparison of annual cycles of modeled monthly mean surface O_3 concentrations with observations at 25 selected surface sites whose locations are plotted in Fig. 1. The observations were mainly taken from the database of the World Data Centre for Greenhouse Gases (WDCGG) (data available at http://gaw.kishou.go.jp/wdcgg/) and the Acid Deposition Monitoring Network in East Asia (EANET) (data available at http://www.eanet.cc/product.html). The O_3 data observed at Chinese mountain sites (Mt. Tai, Mt. Hua, and Mt. Huang) by the collaboration between the Frontier Research Center for Global Change (FRCGC) of the Japan Agency for Marine-Earth Science and Technology (JAMSTEC) and the Institute of Atmospheric Physics (IAP) of the Chinese Academy of Science (CAS) were made available for this comparison (Li et al., 2007). For the comparison in the Southeast Asian region, we used O_3 data obtained at Srinakarin, located in central Thailand (Pochanart et al., 2001). The observation sites for the comparison were chosen to cover the wide longitudinal range of Northern Hemisphere mid-latitudes because the ozone originating from this region has a large impact on the Asian surface O_3 (Wild and Akimoto, 2001; Wild et al., 2004; Sudo and Akimoto, 2007). Only the data observed during the simulation period (2000 to 2005) were compared at each site,

Table 1. Statistical summary of the comparison between the observed and modeled surface O_3 at observational sites shown in Fig. 2[a].

Station Name	Mean (Obs) [ppbv]	Mean (Model) [ppbv]	R	MB [ppbv]	RMSE [ppbv]
Zugspitze-Schneefernerhaus	49.81	50.08	0.97	0.27	1.61
Issyk−Kul	39.54	40.46	0.91	0.92	2.22
Niwot−Ridge−Saddle	52.76	52.14	0.92	−0.62	2.07
Pallas−Sammaltunturi	33.02	30.70	0.77	−2.32	4.16
Hohenpeissenberg	41.05	45.59	0.93	4.54	6.99
Mondy	43.50	40.82	0.83	−2.68	4.44
Mace−Head	37.81	33.57	0.73	−4.24	5.32
Heimaey	39.75	28.43	0.88	−11.32	11.52
Mauna−Loa	40.15	45.35	0.94	5.19	5.46
Trinidad−Head	30.92	30.69	0.72	−0.23	3.44
Tudor−Hill	39.54	36.51	0.98	−3.03	4.02
Angra−do−Heroismo	29.49	34.78	0.88	5.29	6.37
Mt. Tai	56.18	57.34	0.93	1.17	4.52
Mt. Hua	50.29	57.46	0.91	7.18	8.25
Mt. Huang	47.23	51.95	0.79	4.72	7.25
Happo	55.58	47.18	0.95	−8.40	8.99
Rishiri	41.33	36.31	0.80	−5.02	7.25
Ryori	39.06	41.77	0.92	2.71	3.77
Oki	43.00	45.69	0.82	2.69	5.21
Hedo	38.42	38.58	0.98	0.17	4.51
Kanghwa	41.33	48.05	0.89	6.72	7.92
Cheju	36.75	45.95	0.94	9.20	9.54
Ogasawara	28.08	30.74	0.97	2.66	4.00
Srinakarin	27.35	36.53	0.91	9.18	11.03

[a] All statistics are calculated by use of the multiyear averaged monthly means shown in Fig. 2.

except at Srinakarin where only two years (1999 and 2000) of available data were used for comparison.

Table 1 summarizes several statistics of comparison depicted in Fig. 2, presenting the annual mean of the observation and model calculation, correlation coefficient (R), mean bias (MB), and root mean square error (RMSE) between the observations and model calculations. In general, the model successfully represented the seasonal cycle of surface O_3 in both polluted and remote regions. The R values exceeded 0.7 at all sites; in particular, the R values were generally over 0.8 and even over 0.9 for more than half of the East Asian sites. The values of MB and RMSE demonstrated that the absolute concentration of surface O_3 was simulated within a bias of 10 ppbv in most cases. Some details about individual sites are discussed below.

3.1.1 Features of surface O_3 in remote regions

For the remote sites located in inland high-altitude areas (e.g., Zugspitze Schneefernerhause, Niwot Ridge Saddle, and Issyk Kul), the broad summer peak of the surface O_3 was simulated very well. These summer peaks were mainly attributable to the enhanced contribution of O_3 created in the surrounding regions with the leading contribution from the PBL while the stratospheric contribution had a peak of about 20 ppbv in winter to early spring, accounting for half of the total O_3 in that time. At Niwot Ridge Saddle, the model effectively simulated a bulge during July to August in the observations. von Kuhlmann et al. (2003) reported that their model could simulate a similar bulge , but such a bulge was not seen in the observations with which they compared their model results. The data they used might have been observed at the Niwot Ridge C-1 site, which is located about 5 km east and 500 m lower than the Saddle site. The seasonal cycle of O_3 observed at the C-1 site does not display such a bulge in summer as in the Saddle site data. The available observation of surface O_3 at the Saddle site spanned only 15 months from October 2003 to December 2004. Therefore, the bulge might not be a climatological feature but a specific feature in 2004.

Hohenpeissenberg is located close to Zugspitze and shows a distinct broad peak from May to August. The model could simulate this broad summer peak at Hohenpeissenberg, but the magnitude of the peak was overestimated by 5 to 10 ppbv because the model could not represent the smaller daily mean surface O_3, making the range of daily means for the model much narrower than that for the observations. The observatory at Hohenpeissenberg is surrounded by populated areas typical of Central Western Europe; thus, it may suffer from

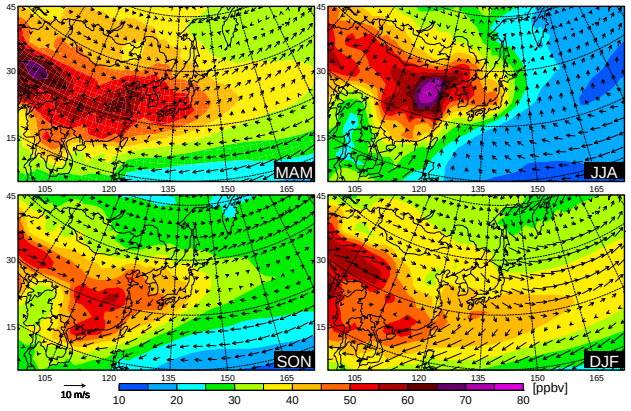

Fig. 3. Simulated seasonal mean surface O_3 (ppbv, colors) and wind vectors (m/s, arrows) in East Asia averaged for the 6 years of the calculation period.

the influence of the NO-titration effect, which cannot be resolved at the horizontal resolution of the current model.

The model effectively simulated the characteristic seasonal cycle with a peak in spring and a trough in summer at the maritime remote sites (Mace Head, Mauna Loa, Heimaey, Trinidad Head, Angra do Heroismo, Tudor Hill, Hedo, and Ogaswara). These spring peaks could be understood as a combination of the stratospheric contribution, which peaks from winter to early spring, and the contribution of the inter- and intracontinental transport of O_3, which peaks in spring. The winter-spring peak of the stratospheric contribution could also be seen in previous global modeling studies (Roelofs et al., 1997; von Kuhlmann et al., 2003), which showed somewhat greater stratospheric contributions than our estimations. A likely cause for the smaller stratospheric contribution in our model was the smaller net flux of O_3 from the stratosphere to the troposphere in our model (120 Tg/yr) than in previous studies ($\sim$500 Tg/yr). This might be due to the O_3 data assimilated in the stratosphere in our model. The data was taken from the output of a stratospheric chemistry model simulation of the last couple of decades (Akiyoshi et al., 2009) and represents the large decline in the lower stratospheric O_3 in the high latitudes of both hemispheres during early 2000s. The summer trough was associated with the summer monsoon that brings low concentrations of O_3 in the marine boundary layer at some East Asian sites (Hedo, Ogasawara, and Srinakarin). The stratospheric contribution generally had a minimum in summer at most sites depicted in Fig. 1, but at sites located in the interior of the Eurasian continent (Mondy and Issyk Kul), the minimum of the stratospheric contribution appeared in autumn.

3.1.2 Seasonal cycles of East Asian surface O_3

Figure 3 illustrates the simulated seasonal mean O_3 concentrations (colors) and wind fields (arrows) at the surface in East Asia and surrounding regions. The belt of the most dense O_3 located between 30° N and 45° N in summer moved southward during winter and then returned northward in summer. This latitudinal movement of the enhanced O_3 belt has also been found in the space-born measurement of tropospheric column O_3 by the Global Ozone Monitoring Experiment (GOME) (Hayashida et al., 2008).

Since the intensity of ultraviolet radiation peaks in summer and hence the chemical production of O_3 also peaks in summer, the surface O_3 over the continental polluted region reaches a maximum in summer. On the other hand, as the North Pacific high pressure system intensifies and expands westward in summer, the clean, unpolluted maritime air mass, which contains less O_3, is transported around the rim of the North Pacific High and flows south-westerly into East Asia. The competition between the influences of these continental and maritime air masses results in several types of seasonal cycles of surface O_3 in East Asian countries. The seasonal behavior of tropospheric O_3 over East Asia has been well documented and analyzed in previous studies (e.g., Pochanart et al., 1999; Naja and Akimoto, 2004; Ding et al., 2008; He et al., 2008; Lin et al., 2009). They discussed the impact of regional pollution (including the effects of biomass burning) and the effect of monsoon circulation on the seasonal changes in East Asian O_3. At two of the mountain sites in China (Mt. Tai and Mt. Hua) depicted in Fig. 2, the peak occurred in June, followed by a small trough in summer, demonstrating that the two sites were strongly influenced by continental air but that a small influence of maritime air in summer was also discernible. Besides the intrusion of maritime air, Lin et al. (2009) discussed the importance of increased cloud cover and rainfall associated with the Asian summer monsoon on the small summer trough of surface O_3 observed at these Chinese mountain sites. In contrast, at another mountain site in China (Mt. Huang), which is located farther south and closer to the ocean, the seasonal cycle of surface O_3 displayed a distinct summer minimum. The model effectively simulated these features of seasonal variation observed at the three mountain sites in China.

The similar distinct summer minimum observed at Mt. Huang could also be seen in the observations at Japanese and South Korean sites (Rishiri, Ryori, Oki, Happo, Hedo, Kanghwa, and Cheju) since both countries lie at the boundary region between continental and maritime air masses. The surface O_3 at these sites had a peak in spring followed by a trough in summer and a second peak in autumn. The model results at these sites showed similar seasonal variations as observed, but the magnitude of the summer troughs was generally underestimated. Thus, the concentrations of O_3 at some of these sites (e.g., Ryori, Oki, Kanghwa, and Cheju) were overestimated in summer. A similar tendency to overestimate summertime O_3 around Japan can be seen in other global model studies (Fiore et al., 2009). Fiore et al. (2009) noticed that the insufficient representation of clean air in the North Pacific High in the model was one possible cause, but the

cause of the insufficient decline of summertime O_3 in our model remains unclear.

For the Japanese mountainous site (Happo), the model underestimated the O_3 throughout the year. The modeled range of the daily mean of the surface O_3 at Happo was apparently biased toward lower concentrations of O_3 compared to the observations, indicating that the model could not well represent the occurrence of high O_3 days. The occurrence of such high concentrations of O_3 might have been influenced by polluted air from the surrounding cities, coupled with the detailed terrain structure and meteorology in the mountainous area, which could not be resolved by the coarse horizontal resolution of the current model.

At the site located in the northern part of Japan (Rishiri), the model underestimated the surface O_3 in winter and spring by about 10 to 15 ppbv. Since the O_3 transported from distant regions contributed significantly in the northern part of Japan in winter to early spring as shown below, the long-range transported O_3 might have been underestimated. The introduction of the reduced dry deposition at a lower temperature had partly eliminated the underestimation, but we still had a discernible underestimation of the surface O_3 in this region. Since anthropogenic emissions in the model (REAS and EDGAR3.2 FT2000) had no seasonal variation, winter heating emissions from Northeast Asia should be underestimated, which might play a role in the model bias during winter and spring.

Although there were some discrepancies between the simulated and observed surface O_3 as noted above, our model had reasonable ability to reproduce the absolute concentrations and seasonal variations of surface O_3 in the Northern Hemisphere mid-latitudes, in particular in the East Asian region, allowing us to analyze the S-R relationship for O_3 in East Asia.

3.2 Contributions to the monthly mean East Asian surface O_3

The upper plot of each figure in Fig. 4 shows the 6-year averaged seasonal evolutions of the monthly mean surface O_3 with contributions from the stratosphere, PBL, and FT, averaged within ten receptor areas within the East Asian region. We set the ten receptor areas as illustrated in the map in Fig. 4: East Japan (JPN-E), West Japan (JPN-W), North Japan (JPN-N), South Japan (JPN-S), North Korea (KOR-N), South Korea (KOR-S), Northeast China (CHN-NE), North China Plain (CHN-NCP), Yangtze River Basin (CHN-YRB), and Southeast China (CHN-SE). The separations of these receptor areas were mainly based on the climatic zone separations used in meteorological studies and statistics (e.g., Liu et al., 2005; Endo and Yasunari, 2006). The difference in the spatial distribution or temporal variation of the meteorological features (e.g., temperature, precipitation, and stream pattern) that define the climatic zone separations probably also affected the spatial distribution or temporal variation of the air pollutants; thus, it was expedient to employ these separations for receptor areas.

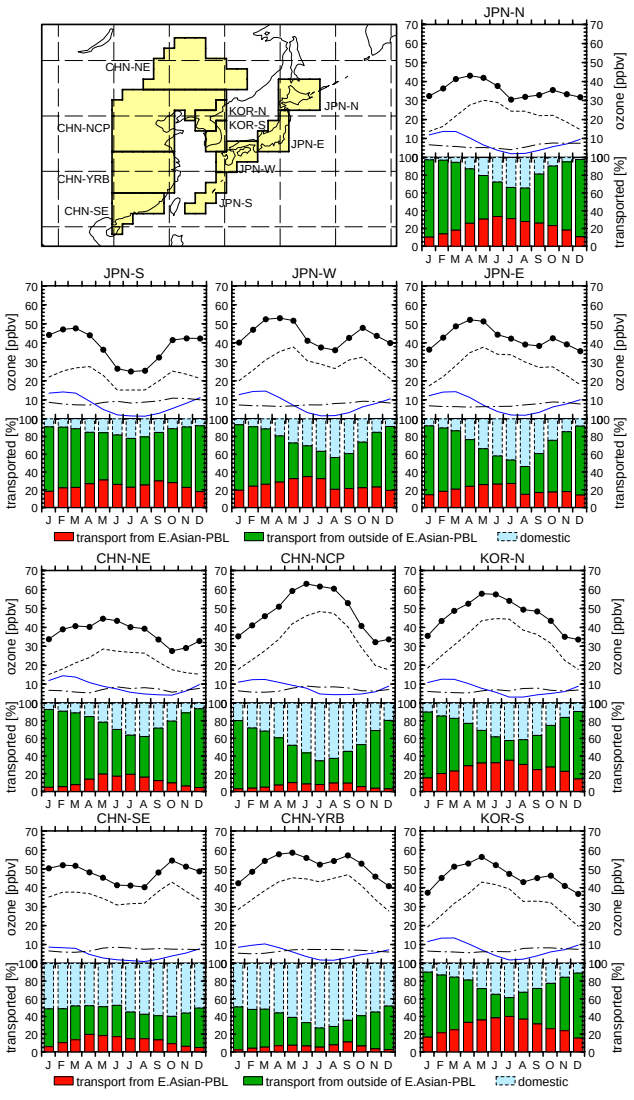

Fig. 4. (Top plots of each figure) Seasonal variations of the area-averaged monthly mean surface O_3 with contributions from the stratosphere (blue solid lines), PBL (black dashed lines), and FT (black dash-dotted lines), calculated by the model. The map shows the areas of averaging. (Bottom plots of each figure) Red bars indicate the contribution (%) of O_3 originating from the PBL in the East Asian source region, green bars from outside of the East Asian PBL, and pale blue bars from domestic pollution (see details in the manuscript). All values are averaged for 6 years.

We saw some mutual features in the seasonal variations of surface O_3 over almost all the receptor areas. First, the contribution of the stratosphere contributed the largest proportion from winter to early spring and reached a minimum in summer. The minimum of the stratospheric contribution in CHN-NE occurred later in autumn, similar to the case of the Eurasian continental sites (Mondy and Issyk Kul) depicted in

Fig. 2. Second, there was a contribution of about 5–10 ppbv originating from the FT year-round with a small seasonal variation having a moderate peak from summer to autumn. On the other hand, the contribution of the PBL showed different seasonal variations depending on the receptor area. It had maxima in spring and autumn in the southern areas (CHN-YRB, CHN-SE, JPN-S), in summer in the northern continental areas (CHN-NCP and CHN-NE), and in spring over most of Japan and the Korean Peninsula.

The lower plot of each figure exhibits the seasonal variation of the relative contribution of transported O_3 from outside of each receptor area. Red bars for each receptor area display the ratio between the total O_3 mixing ratio and the sum of the mixing ratios of O_3 tracers assigned to the PBLs of East Asia and adjacent source regions (CHN, KOR, ECS, JPS, JPN, IDC, and ESB) except the source region including that receptor area. For example, in the case of JPN-N, the summation excluded the PBL of Japan (JPN). Note that for JPN-S, the exception from the summation is not JPN but ECS because the receptor area of JPN-S is located inside the source region of ECS. Green bars indicate a similar ratio, but the sum was taken over the O_3 tracers that were assigned to outside of the PBLs of East Asia and the adjacent source regions. In brief, the red bars for a receptor area indicate the percentage of O_3 originating from the PBL of source regions in East Asia. Strictly, they include the contributions from non-East Asian source regions (IDC, ESB) and exclude the contribution from the PBL source region including that receptor area, but we refer to them as the East Asian contribution for the sake of clarity. The green bars indicate the percentage of O_3 created outside the PBL of the East Asian region, including the FT and stratosphere as well as distant source regions such as Europe or North America, and transported from there. Therefore, the sum of red and green bars for a receptor area indicate the percentage of O_3 transported from all foreign source regions, and consequently the space between the top of green bars and the top transverse, which is shown in pale blue, denotes the percentage of O_3 created in the PBL source region including that receptor area, referred to hereafter as domestic pollution.

As shown in Fig. 4, contributions of O_3 transported from outside of the East Asian PBL became large in the cold season (October to March) and accounted for over 70% of the total O_3 in winter, except in the southern part of China (CHN-YRB, CHN-SE). In the southern part of China, half of the total O_3 was chemically produced in the PBL of the CHN source region, i.e., domestic pollution, even in winter, but in northeast China (CHN-NE), over 80% of the total O_3 was transported from outside of the East Asian PBL, and domestic pollution accounted for less than 10% in the same season. In the cold season, contributions of the stratosphere and the FT were generally large. In particular in winter, the largest part of the O_3 originating from outside the East Asian PBL was due to the stratosphere, and the second largest was the contribution from the FT in every receptor area. The relative contribution of FT in winter was about 20%, mostly consisting of the O_3 created in the non-East Asian FT with a negligible contribution from the East Asian FT (see supplemental Figure S1). In addition to these facts, the contribution of distant PBL source regions, mainly composed of North America (AMN), Europe (EUR), the North Atlantic Ocean (NAT), and Central Asia (CAS), became important in the cold season. The sum of these contributions could exceed 5 ppbv except for southern China, and could even be close to 10 ppbv in CHN-NE (see supplemental Figure S2). Note that the contribution of EUR was largest in early spring (May) in most areas whereas that of AMN was largest in winter. Such a difference in the seasonal dependencies of the contributions was consistent with the previous estimation of the impact from European and North American emission sources on the O_3 concentration in Japan using the emission sensitivity method (Wild and Akimoto, 2001; Wild et al., 2004). In winter, low temperatures and weak ultraviolet (UV) radiation from the sun extended the chemical lifetime of O_3 so that O_3 created in distant source regions could survive the journey to East Asia. Furthermore, the Siberian High established over Eurasia in winter offered an efficient pathway to such O_3 from Europe to Asia (Wild et al., 2004).

In contrast, in the warm season (April to September), the contribution of the O_3 produced in source regions in the East Asian PBL (including domestic pollution) became large while the influence from outside of the East Asian PBL decreased. The O_3 created in the East Asian PBL accounted for about half of the total O_3 in spring and up to about 70% in summer for areas other than CHN-NE and JPN-S. In summer, the relative contribution of the PBL outside East Asia decreased to less than 16%, lower than that of the FT in most receptor areas. The relative contribution of the FT in summer varied by area, ranging from about 12 to 35% with at least one third of it to, in some cases, half of it, originating from the East Asian FT (see supplemental Figure S1). During the warm season, strong UV radiation activated the photochemical reactions relevant to both the formation and destruction of O_3 in the atmosphere so that vigorous chemical production of O_3 took place, but its chemical lifetime also shortened, indicating that O_3 produced in distant regions was mostly lost before reaching the East Asian region. However, a large amount of O_3 could have been created inside the East Asian region and was subject to short range transport such as intracontinental transport inside East Asia before it was chemically lost from the atmosphere.

Figure 5 show the seasonally averaged relative contributions from each source region for spring and summer when the contributions of O_3 chemically produced inside East Asia were generally large. Several contributions with common features were grouped: ASea (Adjacent Sea) is the sum of NPC, JPS, and ECS; IDC+ is the sum of IDC and IND; and RMT (ReMoTe) is the sum of AMN, EUR, CAS, MES, and NAT. The contributions of the East Asian source regions, including domestic pollution, and those of source regions

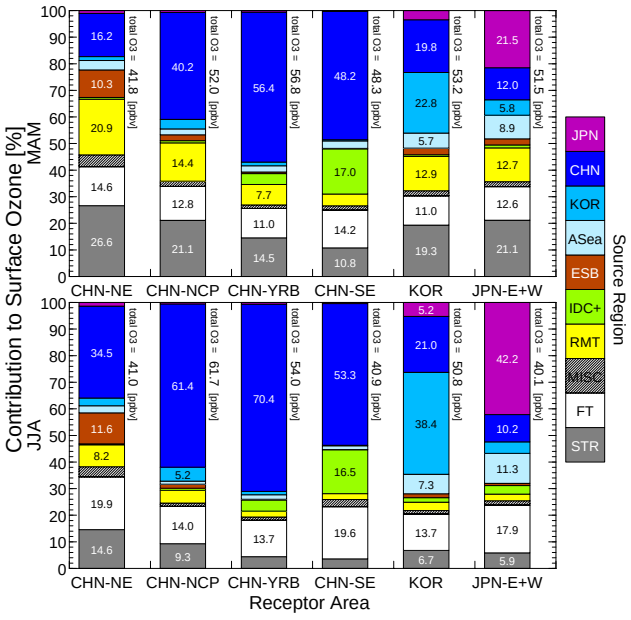

Fig. 5. Seasonal mean relative contribution (%) from source regions to receptor areas in East Asia for spring (top) and summer (bottom). Values are calculated by dividing the seasonal mean contribution (ppbv) from each source region by the seasonal mean total O_3 for each year and averaging for 6 years. Contributions greater than 5% are shown on the bar charts. Six year averaged seasonal mean total O_3 values for each receptor area are shown next to the bar charts. For the source regions: ASea (Adjacent Sea) is the sum of NPC, JPS, and ECS; IDC+ is the sum of IDC and IND, and RMT is the sum of AMN, EUR, CAS, MES, and NAT. For the receptor areas: JPN-E+W is the sum of JPN-E and JPN-W, and KOR is the sum of KOR-N and KOR-S.

outside of the East Asian PBL were comparable in spring, especially in central Japan (JPN-E+W), the Korean Peninsula (KOR), and CHN-NCP while the former well exceeded the latter in the summer.

In every receptor area other than CHN-NE, domestic pollution was the principal contributor to the total O_3 in spring, providing 21.5% in JPN-E+W, 22.8% in KOR, 40.2% in CHN-NCP, and almost half of the total O_3 in the southern part of China (56.4% and 48.2% in CHN-YRB and CHN-SE, respectively). In summer, the share of domestic pollution increased in every receptor area. The share was almost doubled from spring to summer in JPN-E+W (42.2%), KOR (38.4%), and CHN-NE (34.5%), making the domestic contribution dominant, even in CHN-NE.

The springtime stratospheric contribution was around 20% in JPN-E+W and KOR and demonstrated an apparent dependence on latitude in China; its relative contribution increased from south (10.8% in CHN-SE) to north (26.6% in CHN-NE). We saw a similar tendency for the springtime relative contribution of RMT, but its contribution was somewhat less than that from the stratosphere in all receptor regions. The relative contribution from RMT was 12.7% in JPN-E+W and 12.9% in KOR and ranged from below 5% in CHN-SE to 20.9% in CHN-NE. The contributions from the stratosphere were almost halved in every receptor area in summer. Those from RMT underwent a greater reduction from spring to summer of over 50% in every receptor area. The relative contribution of the FT was generally larger in summer than in spring, but in some areas, part of this increase should be attributed to the reduction of the total O_3 from spring to summer, and the absolute contribution was nearly the same, as seen in the upper plots of Fig. 4.

The relative contribution of CHN to KOR and JPN-E+W was similar in both seasons: around 20% and 10% for KOR and JPN-N+W, respectively. The Korean contribution to JPN-E+W was about 6% in spring and less than 5% in summer. The combined relative contribution of CHN and KOR to JPN-E+W in spring, 17.8% as shown in Fig. 5, approximately corresponded to 10 ppbv, consistent with the previous estimation of regional O_3 buildup due to Chinese and Korean sources in spring around Japan (Tanimoto et al., 2005). Due to the dominance of westerly winds, westward transport of O_3 was limited in spring; consequently, the contribution of JPN to KOR or those from JPN and KOR to each receptor area in China were generally small in spring. In summer, the wind direction had no apparent preference for westerly winds as shown in Fig. 3; thus, the westward transport of O_3 occurred somewhat more frequently than in spring. As a result, the contributions from JPN to KOR and from KOR to CHN-NCP accounted for 5.2% of the total O_3 in summer. There were also relatively large contributions of ASea to JPN-E+W and KOR in both seasons. The precursors of ASea O_3 would be originally emitted in the surrounding land area such as China, the Korean Peninsula, or Japan since there are no large emitters in the ocean. In this sense, these maritime contributions should be apportioned to the emission sources on land, and we have to carefully interpret the results. The contributions from East Asian source regions other than ASea presented in Figures 4 and 5 and supplemental Table S1 should be considered as the minimum estimations of the contributions for each source region.

The relative contribution from East Siberia (ESB) was generally large in the northern areas. In CHN-NE, it accounted for about 10.3% and 11.6% of the total O_3 in spring and summer, respectively. The contribution from ESB to CHN-NE peaked in May (∼8 ppbv) and remained almost constant at about 5 ppbv in summer as seen in Fig. S2. In other areas, the relative contribution from ESB was generally larger in spring than in summer. In southern areas in East Asia, the Indochina Peninsula and the Philippines (IDC) and India (IND) provided significant contributions in the warm season. They shared 17.0% of the total O_3 in CHN-SE and nearly 5% in CHN-YRB. In JPN-E+W, relative contributions both from ESB and IDC (+IND) accounted for at most 4% each year even in the warm season. However, their contributions were quite large in JPN-N and JPN-S; the relative

Table 2. Coefficient of variation[a] (%) from the source regions to the receptor areas in East Asia averaged in spring (March-April-May) and summer (June-July-August).

		Receptor Area									
		JPN				KOR		CHN			
		N	E	W	S	N	S	NE	NCP	YRB	SE
Source Region MAM	JPN	12.4	3.7	6.6	25.0	37.9	34.3	25.9	26.5	46.3	51.6
	CHN	13.2	18.4	15.4	10.4	16.1	20.0	3.8	10.8	5.8	6.4
	KOR	18.7	15.5	8.8	16.2	6.3	7.2	5.6	24.8	35.0	33.6
	ASea[b]	8.7	5.8	7.5	6.6	12.3	8.6	14.8	7.8	11.5	17.6
	ESB	12.0	12.9	14.2	18.6	10.6	13.9	9.2	14.1	24.4	33.9
	IDC+[b]	7.6	6.0	7.9	20.0	7.9	5.3	12.0	14.9	21.8	9.7
	RMT[b]	3.5	3.6	10.1	10.5	4.3	7.0	2.8	8.3	13.5	14.0
	MISC	11.1	7.4	6.5	5.4	6.5	5.7	5.5	7.6	5.5	10.9
	FT	4.3	2.9	5.3	4.7	3.4	4.8	3.3	5.5	5.1	5.4
	STR	8.4	10.3	8.5	6.3	9.4	10.0	8.5	9.5	9.6	7.8
	TOTL	4.5	2.0	2.9	3.6	3.5	3.0	1.6	2.9	3.3	4.4
JJA	JPN	11.6	7.0	12.9	53.5	13.1	14.6	30.4	15.8	62.1	80.8
	CHN	22.0	28.7	28.4	27.1	16.6	18.6	6.5	7.6	7.7	10.1
	KOR	25.5	19.3	22.1	64.3	4.4	9.5	17.4	10.9	42.9	92.7
	ASea[b]	8.3	8.0	5.2	9.1	11.0	6.8	26.2	14.7	29.8	44.8
	ESB	30.3	32.2	36.9	55.8	28.3	22.5	10.0	15.4	16.9	43.0
	IDC+[b]	24.8	15.1	20.6	12.3	25.0	19.3	9.4	16.7	23.7	16.9
	RMT[b]	12.7	6.4	10.7	14.7	9.1	13.4	6.8	4.2	12.2	11.3
	MISC	19.7	15.4	8.2	11.9	12.2	9.2	15.6	11.7	10.9	17.2
	FT	6.6	4.3	6.7	6.1	8.2	6.1	7.4	5.6	2.4	4.1
	STR	9.5	3.4	7.7	7.9	7.1	7.6	4.8	4.9	9.2	13.4
	TOTL	3.8	5.3	1.7	3.9	5.0	5.0	3.6	5.1	6.1	5.8

[a] Coefficient of variation is the standard deviation among the annual contributions divided by the 6-year averaged contribution and multiplied by 100.
[b] ASea (Adjacent Sea) is the sum of NPC, JPS, and ECS; IDC+ is the sum of IDC and IND; and RMT (ReMoTe) is the sum of AMN, EUR, CAS, MES, and NAT.

contribution from ESB to JPN-N was about 7% in spring, and that from IDC (+IND) to JPN-S accounted for about 13% in summer.

Table 2 summarizes the interannual variations of the S-R relationship for surface O_3 in East Asia and shows the coefficients of variation of the seasonal means during the six years rather than the standard deviations. Because the seasonal means for spring and summer could differ considerably, the standard deviation was not a good indicator of the interannual variation of the seasonal means.

As the anthropogenic emission data in Asia (REAS) used in this study had interannual trends, it could play a role in the interannual variation of the S-R relationship. However, the main contributor would be the interannual variation in the meteorological conditions. We checked this factor by performing an additional experiment with P and L fixed at the year 2000 but with interannually varied meteorology. The resulted interannual variation of the S-R relationship was similar to the current results, suggesting that the interannual variation in meteorology was the main cause of that in the S-R relationship. This result was also consistent with the findings by Kurokawa et al. (2009), which showed that the interannual variations of springtime O_3 over Japan were largely controlled by the variation in meteorology during the last couple of decades by using the same anthropogenic emission data as used in this study (REAS) with a regional chemical transport model.

The relative interannual variations of the contributions from source regions in East Asia to Japan were generally larger in summer than in spring. This is likely due to the seasonal difference in the meteorological conditions around Japan that transport O_3 from the East Asian source regions to Japan.

The relative interannual variations in the contributions from RMT, FT, and STR to each receptor area in East Asia were generally smaller than those in the contributions from East Asian source regions. The coefficients of variation of the seasonal mean contributions from RMT, FT, and STR

were lower than 15% for spring and summer as well as in autumn and winter (not shown), demonstrating that regions outside of East Asia supply a steady amount of O_3 each year to the East Asian region, which forms a baseline O_3 for East Asia.

The results from this study could be compared with the recent coordinated international effort focused on the intercontinental transport of air pollutants under TF HTAP (Keating and Zuber, 2007; Fiore et al., 2009). Over 20 global scale chemical transport models participating in the HTAP model intercomparison performed a set of coordinated model simulations that included a standard experiment with unperturbed emissions of O_3 precursors, corresponding to the year 2001, and four perturbed experiments with 20% reduction in anthropogenic emissions from East Asia (95° E–160° E, 15° N–50° N), Europe (10° W–50° E, 25° N–65° N), North America (125° W–60° W, 15° N–55° N), and South Asia (50° E–95° E, 5° N–35° N), i.e., the HTAP intercomparison employed the emission sensitivity approach to quantitatively estimate the intercontinental transport between these four regions. Fiore et al. (2009) showed the annual and seasonal mean contributions of Europe and North America to East Asia in their Figure 11 by taking the difference of the calculated O_3 between the standard and perturbed experiments and multiplying it by 5. The median values of the contribution of Europe to East Asia among the HTAP models shown in that figure were about 1.2, 1.1, 1.9, 0.5, and 1.3 ppbv for a year, winter (DJF), spring (MAM), summer (JJA), and autumn (SON), respectively, while those of North America to East Asia were about 1.2, 1.7, 1.4, 0.5, and 1.2 ppbv in the same order. The corresponding contribution values of European sources to East Asia from this study estimated by using the same horizontal definition of the East Asian receptor region as that of the HTAP intercomparison were 1.3, 1.6, 1.7, 0.5, and 1.5 ppbv, and those of the North American source were 1.0, 1.5, 1.1, 0.3, and 1.3 ppbv. The contribution values of each source region to East Asia estimated by our model demonstrated consistent seasonal dependencies with those in the HTAP models and fell within the spread of the HTAP model estimations.

3.3 Hourly mean surface O_3 over Japan: validation and features

Since the current national Ambient Air Quality Standard (AAQS) for O_3 in Japan (60 ppbv) is provided by the hourly mean concentration of O_3, we placed special focus on the hourly mean model output of the surface O_3. Figure 6 compares the simulated and observed seasonal variations of the frequency distribution (FD) of the hourly mean surface O_3 over Japan. Note that these frequencies are area-averaged; frequencies in each model grid are summed to calculate the total frequency in all model grids over Japan and then divided by the number of model grids to form the area-averaged frequency.

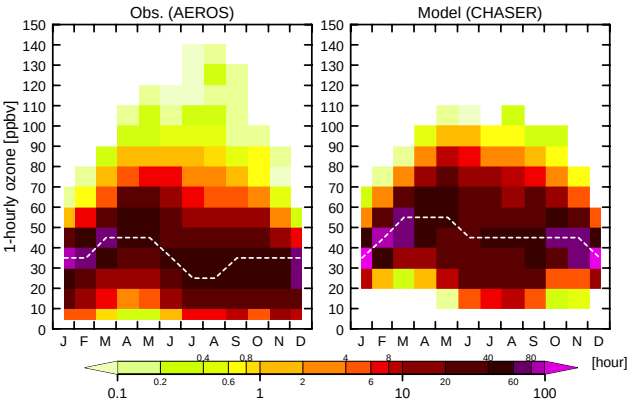

Fig. 6. Seasonal variations of the frequency distributions (FD) of daytime (10:00–16:00) hourly surface O_3 over Japan calculated by use of observations from the Atmospheric Environmental Regional Observation System (AEROS) (left) and model calculations (right). White dotted lines connect the modes of the FDs of each month (ridge line). Monthly FDs are calculated for each year first and then averaged to be shown as 6-year averaged monthly FDs.

We used the hourly surface O_3 data observed at ambient air quality monitoring stations from 2000 to 2005, compiled by the Atmospheric Environmental Regional Observation System (AEROS), for comparison with the model results. About 1,000 monitoring stations are widely distributed throughout Japan except in the southern islands. The monitoring data were averaged in each model grid over Japan; thus, extremely high or low O_3 values in the raw data were smoothed out. Since the horizontal resolution of our model (∼200 km) was not fine enough to simulate the dissipation of O_3 at nighttime due to the NO titration in the ambient atmosphere, the model overestimated the nighttime O_3 mixing ratio in urban areas. Therefore, we selected monitoring data obtained during the daytime, from 10:00 to 16:00, in residential (not mid-urban or industrial) areas for appropriate comparison with the model results. Only daytime O_3 calculated by the model was used for the comparison.

The ridge line of the FD in the observation was the greatest (40–50 ppbv) in spring and decreased to 20–30 ppbv in summer, consistent with the seasonal variation of the monthly mean surface O_3 observed at Japanese monitoring sites shown in Fig. 2. The range of the FD extended toward higher concentrations in summer; thus, the distribution was wider in summer than in spring. In summer, the ridge of the distribution was lowest, but the frequency of the occurrence of a high surface O_3 mixing ratio, such as over 90 ppbv, also increased. As mentioned before, since Japan is largely affected by the intensified North Pacific High in summer, the frequency of observations of low concentrations of O_3 from clean maritime air is increased. However, with the most active photochemical productivity of O_3 also in summer, high concentrations of O_3 could also be produced if the

meteorological conditions become so stable that the precursors of O_3 accumulate and fuel O_3 production in urban areas.

Similar to this observation, the mode of the FD in the model results was the largest concentrations (50–60 ppbv) in spring, and the range of the FD in the model extended toward high O_3 concentrations from the beginning of the year to May. In summer, the mode of the FD in the model decreased compared to that in spring, similar to the observations, but only by 10 ppbv, which was consistent with the overestimation of summertime O_3 in some Japanese observation sites depicted in Fig. 2. It is apparent that the model could not simulate the occurrence of high concentrations of O_3 over 110 ppbv in summer and low concentrations less than 20 ppbv in non-summer seasons. The coarse horizontal resolution may be a cause of the lack of high O_3 events in summer because very dense accumulations of O_3 in urban areas could not be resolved adequately by the 200 km grid spacing. The model fails to simulate the lower O_3 concentrations in non-summer seasons despite limiting the comparison to daytime O_3. Among the observations, very low O_3 (less than 20 ppbv) in daytime typically occurred in the morning and the evening as a transitional stage between the nighttime depleted O_3 and the afternoon maximum. The depleted nighttime O_3 can be observed even in the residual areas. The daytime setting from 10:00 to 16:00 caught this very low O_3 in the morning in the observations. Since the model could not adequately simulate the nighttime O_3 depletion, the very low O_3 in the morning in the transitional stage also could not be simulated with the model.

Although the model could not represent the extremely high O_3 event in summer or the low O_3 in the morning because of its coarse horizontal resolution, the intermediate range that accounts for a large part of the FD of the hourly O_3 could be reasonably simulated with the model. The sufficient hours of occurrence of hourly O_3 over 60 ppbv (Japan's AAQS for O_3) in the model made the analysis of the model's hourly data worthwhile. Thus, we further analyze the hourly data below.

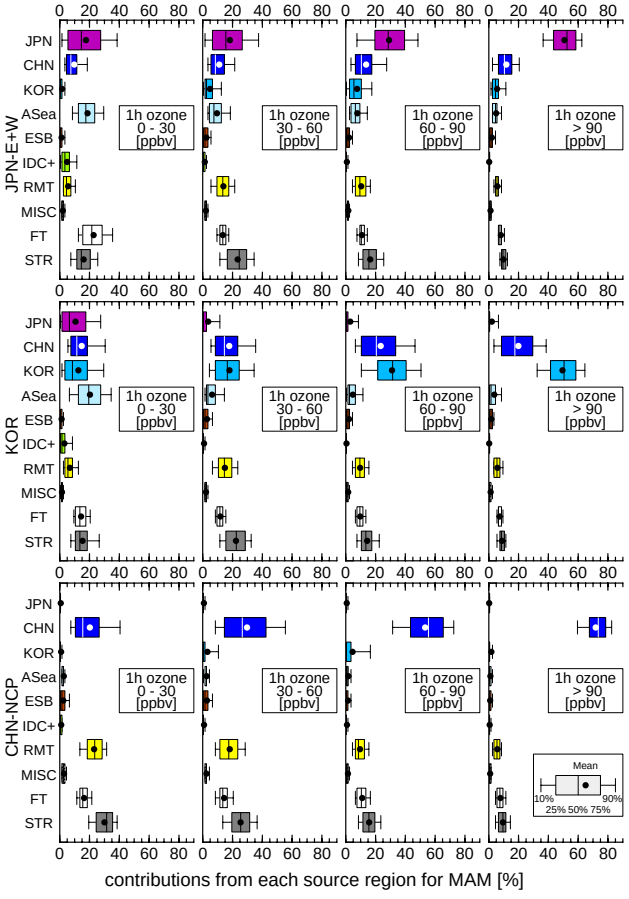

Fig. 7. The hourly relative contributions (%) to the total O_3 from source regions to central Japan (top), the Korean Peninsula (middle), and the North China plain (bottom) for spring (MAM). The box-and-whisker plot represents the 10th, 25th, 50th, 75th, and 90th percentiles of the hourly relative contributions from each source region during the entire 6 year period of calculation, and the black filled circle shows the mean of the hourly relative contributions during the period. All statistics are separately computed for four different classes of total O_3: low (0–30 ppbv), middle (30–60 ppbv), high (60–90 ppbv), and extra-high (>90 ppbv)

3.4 Contributions to the hourly mean surface O_3

Figure 7 shows the hourly relative contributions from each source region in spring, calculated separately for four classes of hourly mean total O_3, low (0–30 ppbv), middle (30–60 ppbv), high (60–90 ppbv), and extra-high (>90 ppbv) concentrations of O_3, for highly populated receptor regions in East Asia at a similar latitude. We calculated the hourly relative contributions by dividing the hourly absolute contributions from each source by the hourly total O_3. Figure 7 shows the mean and the 10th, 25th, 50th, 75th, and 90th percentiles over the entire 6 year period of calculation. The ranges from the 10th to the 90th percentile for several sources were fairly large, often exceeding 30% for the leading sources in particular, indicating that the hourly relative contributions from those source regions could vary considerably. In other words, the S-R relationship for O_3 could vary considerably hour by hour. However, because we intend to discuss the general features of the S-R relationship for O_3 in each O_3 class and elucidate the differences between the O_3 classes, we describe the features and differences mainly based on the mean or median of the hourly relative contributions hereafter.

These plots should be compared to the upper plot of Figure 5 that also shows the relative contributions from each source region in spring but calculated using the monthly mean absolute contributions. For three areas shown in Fig. 7, this "mean" S-R relationship for O_3 depicted in Fig. 5 largely reflects that of the middle (30–60 ppbv) and high (60–90 ppbv) O_3 classes while the S-R relationships for O_3 in the low (0–30 ppbv) and extra-high (>90 ppbv) O_3 classes were

fairly different from the mean S-R relationship. The relative contribution from domestic pollution became increasingly dominant in the higher O_3 classes. In the extra-high O_3 class, the relative contribution of domestic pollution roughly accounted for 50%, 50%, and 70% of the total O_3 in JPN-E+W, KOR, and CHN-NCP, respectively. In the low O_3 class, domestic pollution was no longer the principal component of surface O_3 in every receptor area; instead, large contributions originated from source regions that did not have leading contributions in the mean S-R relationship for O_3. The influences of ASea and FT became predominant in JPN-E+W whereas ASea and JPN had greater contributions than in the mean S-R relationship in KOR. In CHN-NCP, the mean and median of the domestic contribution were overtaken by those of RMT or the stratosphere in the low O_3 class.

The S-R relationship for O_3 among the three main East Asian countries could vary according to the rank of O_3. The mean relative contribution from CHN to JPN-E+W was around 10% in every class of O_3 with the 10th–90th percentile of the relative contribution ranging from a couple of percents to about 20% (up to 30% in the high O_3 class). On the other hand, the relative contribution from KOR was almost negligible in the low O_3 class, but its range of distribution widened in the higher O_3 classes, and the relative contribution occasionally exceeded 10% in the middle O_3 class, reaching almost 20% in the high O_3 class. The contribution of CHN to KOR was large and comparable to that of domestic pollution in the low and middle O_3 classes. In the high O_3 class, CHN had a large influence on KOR; the 10th–90th percentile range of the relative contribution from CHN and that from domestic pollution overlapped considerably. In the extra-high O_3 class, the contribution of CHN to KOR was generally larger than that to JPN-E+W. Since CHN-NCP is located upwind of Japan and the Korean Peninsula in spring, the influences of those regions on CHN-NCP were generally small with an occasional large contribution from KOR in the middle and high O_3 classes. Therefore, for CHN-NCP, the contribution of RMT, which included central Asia (CAS) located upwind of China, was the second largest among the source regions in the PBL after the PBL of CHN.

The relative contribution of RMT to CHN-NCP gradually decreased as the class of O_3 increased, but the absolute contribution stayed approximately constant at 6–8 ppbv in every O_3 class. Similarly, the absolute contributions of the FT and STR were 5–8 ppbv and 9–11 ppbv, respectively. Note that the absolute contributions of RMT, FT, and STR to JPN-E+W and KOR were very similar to those to CHN-NCP except in the low O_3 class. We also saw the similarities among the absolute contributions of the RMT, FT, and STR to these East Asian receptor areas in other seasons, demonstrating that such source regions outside of East Asia provided a baseline for O_3 in East Asia year-round.

Similar features of the relative contributions from each source region in each class of O_3 were evident in summer although the respective values of the contributions were different. In general, the contribution of domestic pollution intensified, and those of the STR and RMT declined for every O_3 class.

For the class of O_3 over 60 ppbv (Japan's AAQS), domestically produced O_3 provided the principal contribution in both the high and extra-high O_3 classes to central Japan (JPN-E+W). Table 3 summarizes the mean absolute and relative contributions from each source region to central Japan in the high and extra-high O_3 classes in spring and summer. The domestic contribution was smaller in the high O_3 class than in the extra-high O_3 class during both seasons. In contrast, the relative contributions from foreign sources were generally greater in the high O_3 class than in the extra-high O_3 class, reflecting the fact that the absolute contribution from each foreign source remained rather constant between both O_3 classes in each season. The approximate numbers of the absolute contribution from leading foreign sources were as follows in spring and summer, respectively: CHN (10 ppbv, 8 ppbv), KOR (5 ppbv, 6 ppbv), ASea (5 ppbv, 5 ppbv), RMT (6 ppbv, 2 ppbv), FT (7.5 ppbv, 7.5 ppbv), and STR (10 ppbv, 5 ppbv). These model results suggested that the impact of foreign sources on Japan's AAQS was the most critical in the high O_3 class (60–90 ppbv) in spring. For the same O_3 class in summer, absolute contributions from East Asian foreign sources were nearly the same as in spring, and those from the intercontinental transport (RMT) and the stratosphere decreased relative to spring.

4 Summary and conclusions

In this study, we quantitatively estimated the proportion of surface O_3 over several receptor areas in East Asia that is attributable to source regions in the global atmosphere, i.e. the S-R relationship for surface O_3 in East Asia, for the early 2000s through a multiyear simulation using the global chemical transport model CHASER with the tracer tagging method. We investigated the S-R relationship for surface O_3 in East Asia with special focus on the role of intracontinental transport of O_3 within East Asia as well as the transport of O_3 from distant regions. The differences in the S-R relationship for O_3 in different classes of hourly O_3 concentrations were also discussed.

We evaluated the modeled surface O_3 through comparison with observations over an extensive longitudinal range in the Northern Hemisphere mid-latitudes. The model well simulated several characteristic seasonal variations of surface O_3, such as the broad summer peaks at inland mountainous areas and the spring peaks and summer minimums at the remote maritime sites. Although there were some quantitative problems with as yet unidentified causes at several sites, the model properly reproduced the regional differences in the seasonal transitions of surface O_3 in East Asia.

Our simulation demonstrated the significant seasonal differences in the origin of surface O_3 in East Asia. O_3

Table 3. The mean hourly contributions from source regions to central Japan (JPN-E+W) in the high O_3 (60–90 ppbv) and extra-high O_3 (>90 ppbv) classes for spring (MAM) and summer (JJA)[a,b].

	Mean contribution from source regions to central Japan, ppbv (%)							
	MAM				JJA			
Regions	60–90		> 90		60–90		> 90	
JPN	19.8	(29.0)	47.4	(50.8)	34.6	(50.5)	55.9	(59.8)
CHN	9.1	(13.6)	11.0	(11.8)	7.6	(11.1)	8.9	(9.6)
KOR	5.1	(7.6)	5.2	(5.6)	5.1	(7.4)	7.1	(7.6)
ASea	5.2	(7.7)	4.6	(4.9)	5.4	(8.0)	4.7	(5.1)
ESB	1.5	(2.2)	1.9	(2.1)	0.8	(1.1)	1.0	(1.0)
IDC+	0.5	(0.7)	0.2	(0.2)	0.8	(1.3)	0.4	(0.5)
RMT	6.8	(10.3)	5.3	(5.7)	1.8	(2.7)	2.2	(2.4)
MISC	1.1	(1.7)	1.0	(1.1)	0.7	(1.1)	0.6	(0.7)
FT	7.2	(10.8)	7.5	(8.1)	7.5	(11.1)	7.6	(8.1)
STR	10.8	(16.4)	9.1	(9.8)	4.0	(5.8)	5.0	(5.3)

[a] Values are given in ppbv.
[b] Values in brackets denote relative contributions in %.

transported from outside of the East Asian PBL with leading contributions from the stratosphere, free troposphere, Europe, North America, North Atlantic, and Central Asia accounted for the largest portion of surface O_3 (over 70%) in winter, except in southern China. In contrast, the share of O_3 created in East Asia reached 50% in spring and further increased to around 70% in summer in most areas of East Asia. The main component of this O_3 was domestic in origin, accounting for over 20% and 40% of the total O_3 in the spring and summer, respectively, in most areas. We estimated the relative contribution of China to Japan and the Korean Peninsula to be about 10% and 20%, respectively, and the Korean contribution to Japan was around 5% in the warm season. The contribution from East Siberia to Northeast China accounted for about 10%, and that from the Indochina Peninsula to Southeast China was about 17%. The relative contribution of intercontinental transport from distant sources in spring was the greatest in Northeast China (21%) and about 13% in the Korean Peninsula and Japan. The interannual difference in this S-R relationship for O_3 was generally small for distant sources (<15%) but was sometimes large for East Asian sources, particularly during summer.

We analyzed air quality monitoring data over Japan to demonstrate the seasonal variation of the frequency distribution of the hourly mean surface O_3. The most frequently observed O_3 concentration was 40–50 ppbv in spring, decreasing to 20–30 ppbv in summer. The frequency of occurrence of extra-high O_3 (over 90 ppbv) increased in summer, making the range of the frequency distribution wider in summer than in spring. The model could not thoroughly simulate all these observed features in the frequency distribution, but some of them, including the highest mode value in spring, were represented in the model.

We showed the difference in the S-R relationship for O_3 estimated separately according to the class of the hourly total O_3 concentration in spring. In every O_3 class except the lowest (<30 ppbv), domestic pollution was the main contributor and its share increased in the higher O_3 classes: over 50% in the extra-high O_3 class (>90 ppbv). The mean relative contribution to central Japan from China was about 10% for every class of O_3, but that from the Korean Peninsula became significant only for the middle and higher O_3 classes (>30 ppbv). We estimated that China had a large impact, almost comparable to domestic pollution, on O_3 concentrations in the Korean Peninsula except for the extra-high O_3 class (>90 ppbv). In contrast, China received relatively little O_3 from Japan or the Korean Peninsula in spring. Sources outside of the East Asian PBL, including the stratosphere, free troposphere, Europe, North America, North Atlantic, and Central Asia, contributed steady amounts of O_3 to East Asia for every O_3 class during each season, constituting the baseline O_3 in East Asia. The model results suggested that the impact of such foreign sources on Japan's AAQS was the most critical in the high O_3 class (60–90 ppbv) in spring.

Supplement related to this article is available online at: http://www.atmos-chem-phys.net/10/11305/2010/acp-10-11305-2010-supplement.pdf.

Acknowledgements. We thank two anonymous reviewers for their helpful comments. This research was supported by the Global Environment Research Fund (C-081 and S-7) by the Ministry of the Environment (MOE), Japan, and the Asian Environment Research Program at the National Institute for Environmental Studies (NIES). We would like to acknowledge the entire staff of the EANET and the air quality monitoring stations of the MOE

and of the local governments for carrying out measurements and providing the observations. We thank the NOAA Earth System Research Laboratory, Global Monitoring Division; German Meteorological Service, Hohenpeissenberg Meteorological Observatory; Instituto de Meteorologia, Portugal; Japan Meteorological Agency; National University of Ireland; Finnish Meteorological Institute; Environment Canada, Air Quality Research Branch; Federal Environmental Agency, Germany; and Kyrgyz National University for providing ground-based ozone data through the WDCGG data base. We thank P. Pochanart for providing the surface O_3 data of the Chinese mountain sites that we obtained through the GERF (B-051) by the MOE. The calculations were performed on the NIES supercomputer system (NEC SX-8R). The GFD-DENNOU library was used for drawing the figures.

Edited by: P. Monks

References

Akiyoshi, H., Zhou, L. B., Yamashita, Y., Sakamoto, K., Yoshiki, M., Nagashima, T., Takahashi, T., Kurokawa, J., Takigawa, M., and T. Imamura, T.: A CCM simulation of the breakup of the Antarctic polar vortex in the years 1980–2004 under the CCMVal scenarios, J. Geophys. Res., 114, D03103, doi:10.1029/2007JD009261, 2009.

Auvray, M. and Bey, I.: Long-range transport to Europe: Seasonal variations and implications for the European ozone budget, J. Geophys. Res., 110, D11303, doi:10.1029/2004JD005503, 2005.

Brasseur, G. P., Orlando, J. J., and Tyndall, G. S. (Eds.): Atmospheric chemistry and global change, Topics in environmental chemistry, Oxford University Press, New York, USA, 1999.

Chang, S.-C. and Lee, C. T.: Evaluation of the trend of air quality in Taipei, Taiwan from 1994 to 2003, Environ. Monit. Assess., 127, 87–96, 2007.

Carmichael, G. R., Calori, G., Hayami, H., Uno, I., Cho, S. Y., Engardt, M., Kim, S. B., Ichikawa, Y., Ikeda, Y., Woo, J. H., Ueda, H., and Amann, M.: The MICS-Asia study: model intercomparison of long-range transport and sulfur deposition in East Asia, Atmos. Environ., 36, 175–199, 2002.

Chou, C. C.-K., Liu, S. C., Lin, C.-Y., Shiu, C.-J., and Chang, K.-H.: The trend of surface ozone in Taipei, Taiwan, and its causes: Implications for ozone control strategies, Atmos. Environ., 40, 3898–3908, 2006.

Derwent, R. G., Stevenson, D. S., Collins, W. J., and Johnson, C. E.: Intercontinental transport and the origins of the ozone observed at surface sites in Europe, Atmos. Environ., 38, 1891–1901, 2004.

Ding, A. J., Wang, T., Thouret, V., Cammas, J.-P., and Nedelec, P.: Tropospheric ozone climatology over Beijing: analysis of aircraft data from the MOZAIC program, Atmos. Chem. Phys., 8, 1–13, doi:10.5194/acp-8-1-2008, 2008.

Emori, S., Nozawa, T., Numaguti, A., and Uno, I.: Importance of cumulus parameterization for precipitation simulation over East Asia in June, J. Meteorol. Soc. Jpn., 79, 939–947, 2001.

Endo, N. and Yasunari, T.: Changes in low cloudiness over China between 1971 and 1996, J. Climate., 19, 1204–1213, 2006.

Fiore, A. M., Jacob, D. J., Bey, I., Yantosca, Y. M., Field, B. D., Fusco, A. C., and Wilkinson, J. G.: Background ozone over the United States in summer: Origin, trend, and contribution to pollution episodes, J. Geophys. Res., 107(D15), 4275, doi:10.1029/2001JD000982, 2002.

Fiore, A. M., Dentener, F. J., Wild, O., Cuvelier, C., Schultz, M. G., Hess, P., Textor, C., Schulz, M., Doherty, R. M., Horowitz, L. W., MacKenzie, I. A., Sanderson, M. G., Shindell, D. T., Stevenson, D. S., Szopa, S., van Dingenen, R., Zeng, G., Atherton, C., Bergmann, D., Bey, I., Carmichael, G., Collins, W. J., Duncan, B. N., Faluvegi, G., Folberth, G., Gauss, M., Gong, S., Hauglustaine, D., Holloway, T., Isaksen, I. S. A., Jacob, D. J., Jonson, J. E., Kaminski, J. W., Keating, T. J., Lupu, A., Marmer, E., Montanaro, V., Park, R. J., Pitari, G., Pringle, K. J., Pyle, J. A., Schroeder, S., Vivanco, M. G., Wind, P., Wojcik, G., Wu, S., and Zuber, A. : Multimodel estimates of intercontinental source-receptor relationships for ozone pollution, J. Geophys. Res., 114, D04301, doi:10.1029/2008JD010816, 2009.

Hayashida, S., Urita, N., Noguchi, K., Liu, X., and Chance, K.: Spatiotemporal Variation in Tropospheric Column Ozone over East Asia Observed by GOME and Ozonesondes, SOLA, 4, 117–120, doi:10.2151/sola.2008-030, 2008.

He, Y. J., Uno, I., Wang, Z. F., Pochanart, P., Li, J., and Akimoto, H.: Significant impact of the East Asia monsoon on ozone seasonal behavior in the boundary layer of Eastern China and the west Pacific region, Atmos. Chem. Phys., 8, 7543–7555, doi:10.5194/acp-8-7543-2008, 2008.

Hess, P. G. and Lamarque, J.-F.: Ozone source attribution and its modulation by the Arctic oscillation during the spring months, J. Geophys. Res., 112, D11303, doi:10.1029/2006JD007557, 2007.

Irie, H., Sudo, K., Akimoto, H., Richter, A., Burrows, J. P., Wagner, T., Wenig, M., Beirle, S., Kondo, Y., Sinyakov, V. P., and Goutail, F.: Evaluation of long-term tropospheric NO_2 data obtained by GOME over East Asia in 1996–2002, Geophys. Res., Lett., 32, L11810, doi:10.1029/2005GL022770, 2005.

Jacob, D. J., Logan, J. A., and Murti, P. P.: Effect of rising Asian emissions on surface ozone in the United States, Geophys. Res. Lett., 26(14), 2175–2178, 1999.

Kalnay, E., Kanamitsu, M., Kistler, R., Collins, W., Deaven, D., Gandin, L., Iredell, M., Saha, S., White, G., Woollen, J., Zhu, Y., Leetmaa, A., Reynolds, R., Chelliah, M., Ebisuzaki, W., Higgins, W., Janowiak, J., Mo, K. C., Ropelewski, C., Wang, J., Jenne, R., and Joseph, D.: The NCEP/NCAR 40-year reanalysis project, Bull. Amer. Meteor. Soc., 77, 437–470, 1996.

Kanaya, Y., Pochanart, P., Liu, Y., Li, J., Tanimoto, H., Kato, S., Suthawaree, J., Inomata, S., Taketani, F., Okuzawa, K., Kawamura, K., Akimoto, H., and Wang, Z. F.: Rates and regimes of photochemical ozone production over Central East China in June 2006: a box model analysis using comprehensive measurements of ozone precursors, Atmos. Chem. Phys., 9, 7711–7723, doi:10.5194/acp-9-7711-2009, 2009.

Keating, T. J. and Zuber A. (Eds.): Hemispheric transport of air pollution 2007 interim report, Air Pollut. Stud. No. 16, U. N. Econ. Comm. for Europe, Geneva, 2007.

Kobayashi, K.: Assessing the impacts of tropospheric ozone on agricultural production. J. Jpn. Soc. Atmos. Environ., 34, 162–175, (in Japanese with English summary), 1999.

Kurokawa, J., Ohara, T., Uno, I., Hayasaki, M., and Tanimoto, H.: Influence of meteorological variability on interannual variations of springtime boundary layer ozone over Japan during 1981–2005, Atmos. Chem. Phys., 9, 6287–6304, doi:10.5194/acp-9-6287-2009, 2009.

Li, J., Wang, Z. F., Akimoto, H., Gao, C., Pochanart, P., and Wang, X.: Modeling study of the seasonal cycle of ozone in the boundary layer over East Asia, J. Geophys. Res., 112, D22S25, doi:10.1029/2006JD008209, 2007.

Li, J., Wang, Z. F., Akimoto, H., Yamaji, K., Takigawa, M., Pochanart, P., Liu, Y., Tanimoto, H., and Kanaya, Y.: Near-ground ozone source attributions and outflow in central eastern China during MTX2006, Atmos. Chem. Phys., 8, 7335–7351, doi:10.5194/acp-8-7335-2008, 2008.

Li, Q., Jacob, D. J., Bey, I., Palmer, P. I., Duncan, B. N., Field, B. D., Martin, R. V., Fiore, A. M., Yantosca, R. M., Parrish, D. D., Simmonds, P. G., and Oltmans, S. J.: Transatlantic transport of pollution and its effects on surface ozone in Europe and North America, J. Geophys. Res., 107(D13), 4166, doi:10.1029/2001JD001422, 2002.

Lin, M., Oki, T., Bengtsson, M., Kanae, S., Holloway, T., and Streets, D. G.: Long-range transport of acidifying substances in East Asia—Part II Source–receptor relationships, Atmos. Environ., 42, 5956–5967, 2008.

Lin, M., Holloway, H., Oki, T., Streets, D. G., and Richter, A.: Multi-scale model analysis of boundary layer ozone over East Asia, Atmos. Chem. Phys., 9, 3277–3301, 2009, http://www.atmos-chem-phys.net/9/3277/2009/.

Lin, S.-J. and Rood, R. B.: Multidimensional flux-form semi-Lagrangian transport scheme, Mon. Weather Rev., 124, 2046–2070, 1996.

Liu, B., Xu, M., Henderson, M., and Qi, Y.: Observed trends of precipitation amount, frequency, and intensity in China, 1960–2000, J. Geophys. Res., 110, D08103, doi:10.1029/2004JD004864, 2005.

Lu, W.-Z. and Wang, X.-K.: Evolving trend and self-similarity of ozone pollution in central Hong Kong ambient during 1984–2002, Science of the Total Environment, 357, 160–168, 2006.

Ministry of Environment (MOE) Japan: FY 2008 status of air pollution, available online at: http://www.env.go.jp/air/osen/jokyo_h20/, (in Japanese), 2008.

Naja, M. and Akimoto, H.: Contribution of regional pollution and long-range transport to the Asia-Pcific region: Analysis of long-term ozonesonde data over Japan, J. Geophys. Res., 109, D21306, doi:10.1029/2004JD004687, 2004.

Numaguti, A., Takahashi, M., Nakajima, T., and Sumi, A.: Development of an atmospheric general circulation model, in Matsuno, T. ed., Climate system dynamics and modering, Vol. I-3 of Reports of A New Program for Creative Basic Research Studies: Studies of Global Environmental Change with special reference to Asia and Pacific Regions, Tokyo, Center for Climate System Research, University of Tokyo, 1–27, 2005.

Ohara, T. and Sakata, T.: Long-term variation of photochemical oxidants over Japan, J. Jpn. Soc. Atmos. Environ., 38, 47–54, (in Japanese with English summary), 2003.

Ohara, T., Akimoto, H., Kurokawa, J., Horii, N., Yamaji, K., Yan, X., and Hayasaka, T.: An Asian emission inventory of anthropogenic emission sources for the period 1980–2002, Atmos. Chem. Phys., 7, 4410–4444, doi:10.5194/acp-7-4410-2007, 2007.

Olivier, J. G. J. and Berdowski, J. J. M.: Global emissions sources and sinks, in: The Climate System, Berdowski, J., Guicherit, R., and Heij, B. J. (eds.), A. A. Balkema Publishers/Swets & Zeitlinger Publishers, Lisse, The Netherlands, 33–78, 2001.

Pochanart, P., Kreasuwun, J., Sukasem, P., Geeratithadaniyom, W., Tabucanon, M. S., Hirokawa, J., Kajii, Y., and Akimoto, H.: Tropical tropospheric ozone observed in Thailand, Atmos. Environ., 35, 2657–2668, 2001.

Pochanart, P., Hirokawa, J., Kajii, Y., Akimoto, H., and Nakao, M.: Influence of regional-scale anthropogenic activity in northeast Asia on seasonal variations of surface ozone and carbon monoxide observed at Oki, Japan, J. Geophys. Res., 104(D3), 3621–3631, 1999.

Rayner, N. A., Parker, D. E., Horton, E. B., Folland, C. K., Alexander, L. V., Rowell, D. P., Kent, E. C., Kaplan, A.: Global analyses of sea surface temperature, sea ice, and night marine air temperature since the late nineteenth century, J. Geophys. Res., 108(D14), 4407, doi:10.1029/2002JD002670, 2003.

Richter, A., Burrows, J. P., Nues, H., Grainer, C., and Niemeijer, U.: Increase in tropospheric nitrogen dioxide over China observed from space, Nature, 437, 129–132, 2005.

Roelofs, G.-J., Lelieveld, J., and van Dorland, R.: A three-dimensional chemistry/general circulation model simulation of anthropogenically derived ozone in the troposphere and its radiative climate forcing, J. Geophys. Res., 102(D19), 23389–23401, 1997.

Schultz, M. G., Heil, A., Hoelzemann, J. J., Spessa, A., Thonicke, K., Goldammer, J. G., Held, A. C., Pereira, J. M. C., and van het Bolscher, M.: Global wildland fire emissions from 1960 to 2000, Global Biogeochem. Cycles, 22, GB2002, doi:10.1029/2007GB003031, 2008.

Stevenson, D. S., Dentener, F. J., Schultz, M. G., Ellingsen, K., van Noije, T. P. C., Wild, O., Zeng, G., Amann, M., Atherton, C. S., Bell, N., Bergmann, D. J., Bey, I., Butler, T., Cofala, J., Collins, W. J., Derwent, R. G., Doherty, R. M., Drevet, J., Eskes, H. J., Fiore, A. M., Gauss, M., Hauglustaine, D. A., Horowitz, L. W., Isaksen, I. S. A., Krol, M. C., Lamarque, J.-F., Lawrence, M. G., Montanaro, V., Muller, J.-F., Pitari, G., Prather, M. J., Pyle, J. A., Rast, S., Rodriguez, J. M., Sanderson, M. G., Savage, N.H., Shindell, D. T., Strahan, S. E., Sudo, K., and Szopa, S.: Multimodel ensemble simulations of present-day and near-future tropospheric ozone, J. Geophys. Res., 111, D08301, doi:10.1029/2005JD006338, 2006.

Sudo, K. and Akimoto, H.: Global source attribution of tropospheric ozone: Long-range transport from various source regions, J. Geophys. Res., 112, D12302, doi:10.1029/2006JD007992, 2007.

Sudo, K., Takahashi, M., Kurokawa, J., and Akimoto, H.: CHASER: A global chemical model of the troposphere: 1. Model description, J. Geophys. Res., 107(D17), 4339, doi:10.1029/2001JD001113, 2002a.

Sudo, K., Takahashi, M., and Akimoto, H.: CHASER: A global chemical model of the troposphere: 2 Model results and evaluation, J. Geophys. Res., 107(D17), 4586, doi:10.1029/2001JD001114, 2002b.

Takigawa, M., Takahashi, M., and Akiyoshi, H.: Simulation of ozone and other chemical species using a Center for Climate System Research/National Institute for Environmental Studies atmospheric GCM with coupled stratospheric chemistry, J. Geophys. Res., 104, 14003–14018, 1999.

Tanimoto, H., Sawa, Y., Matsueda, H., Uno, I., Ohara, T., Yamaji, K., Kurokawa, J., and Tonemura, S.: Significant latitudinal gradient in the surface ozone spring maximum over East Asia, Geo-

phys. Res. Lett., 32, L21805, doi:10.1029/2005GL023514, 2005.
Tanimoto, H: Increase in springtime tropospheric ozone at a mountainous site in Japan for the period 1998–2006, Atmos. Environ., 43, 1358–1363, 2009.
US Environmental Protection Agency: Air Quality Criteria for Ozone and Related Photochemical Oxidants (Final), US Environmental Protection Agency, Washington, DC, USA, EPA/600/R-05/004aF-cF, 2006.
van Leer, B.: Toward the ultimate conservative difference scheme. Part IV: A new approach to numerical convection, J. Comput. Phys., 23, 276–299, 1977.
von Kuhlmann, R., Lawrence, M. G., Crutzen, P. J., and Rasch, P. J.: A model for studies of tropospheric ozone and nonmethane hydrocarbons: Model descriptions and ozone results, J. Geophys. Res., 108(D9), 4294, doi:10.1029/2002JD002893, 2003.
Wang, H., Kiang, C. S., Xiaoyan, T., Xiuji, Z., and Chameides, W. L.: Surface ozone: A likely threat to crops in Yangtze delta of China, Atmos. Environ., 39, 3843–3850, 2005.
Wang, T., Wei, L., Ding, A. J., Poon, C. N., Lam, K. S., Li, Y. S., Chan, L. Y., and Anson, M.: Increasing surface ozone concentrations in the background atmosphere of Southern China, 1994–2007, Atmos. Chem. Phys., 9, 6217–6227, doi:10.5194/acp-9-6217-2009, 2009.
Wang, Y., Jacob, D. J., and Logan, J. A.: Global simulation of tropospheric O3-NOx-hydrocarbon chemistry: 3. Origin of tropospheric ozone and effects of nonmethane hydrocarbons, J. Geophys. Res., 103(D9), 10757–10767, 1998.
Wesely, M. L.: Parameterization of surface resistance to gaseous dry deposition in regional-scale numerical models, Atmos. Environ., 23, 1293–1304, 1989.
Wild, O.: Modelling the global tropospheric ozone budget: exploring the variability in current models, Atmos. Chem. Phys., 7, 2643–2660, doi:10.5194/acp-7-2643-2007, 2007.
Wild, O. and Akimoto, H.: Intercontinental transport of ozone and its precursors in a three-dimensional global CTM, J. Geophys. Res., 106(D21), 27729–27744, 2001.
Wild, O., Pochanart, P., and Akimoto, H.: Trans-Eurasian transport of ozone and its precursors, J. Geophys. Res., 109, D11302, doi:10.1029/2003JD004501, 2004.
Xu, X., Lin, W., Wang, T., Yan, P. Tang, J., Meng, Z., and Wang, Y.: Long-term trend of surface ozone at regional background station in eastern China 1991–2006: enhanced variability, Atmos. Chem. Phys., 8, 2595–2607, doi:10.5194/acp-8-2595-2008, 2008.